Title Page

Heterogeneous distribution of *Fusobacterium nucleatum* in the progression of colorectal cancer

Shumpei Yamamoto[1], Hideaki Kinugasa*[,1], Mami Hirai[1], Hiroyuki Terasawa[1], Eriko Yasutomi[1], Shohei Oka[1], Masayasu Ohmori[1], Yasushi Yamasaki[1], Toshihiro Inokuchi[1], Keita Harada[1], Sakiko Hiraoka[1], Kazuhiro Nouso[1], Takehiro Tanaka[2], Fuminori Teraishi[3], Toshiyoshi Fujiwara[3], and Hiroyuki Okada[1]

[1]Department of Gastroenterology and Hepatology, [2]Department of Pathology, [3]Department of Gastroenterological Surgery, Okayama University Graduate School of Medicine, Dentistry, and Pharmaceutical Sciences, 2-5-1 Shikata-cho, Kita-ku, Okayama-city, Okayama, 700-8558 Japan

Tel: +81-86-235-7219, FAX: +81-86-225-5991,

Corresponding author: Hideaki Kinugasa; E-mail: gyacy14@gmail.com

Running head: Heterogeneous Fusobacterium in colorectal cancer

Conflict of interest

The authors have no conflicts of interest to declare.

Acknowledgements

This study was supported by japanese society for the promotion of science KAKENHI (19k17433.)

Title: Heterogeneous distribution of *Fusobacterium nucleatum* in the progression of colorectal cancer

Abstract

Background and Aim

Fusobacterium nucleatum (*Fn*) is involved in colorectal cancer (CRC) growth and is a biomarker for patient prognosis and management. However, the ecology of *Fn* in CRC and the distribution of intratumoral *Fn* are unknown.

Methods

We evaluated *Fn*, and the status of KRAS and BRAF in 200 colorectal neoplasms (118 adenomas and 82 cancers) and 149 matched adjacent normal mucosas. The differentiation status between "surface" and "deep" areas of cancer tissue and matched normal mucosa were analyzed in 46 surgical samples; the Ki-67 index was also evaluated in these samples.

Results

Fn presence in the tumor increased according to pathological stage: 5.9% (adenoma) to 81.8% (stage III/IV), while *Fn* presence in normal mucosa also increased: 7.6% (adenoma) to 40.9% (stage III/IV). The detection rates of *Fn* on the tumor surface and in deep areas were 45.7% and 32.6%, while that of normal mucosa was 26.1% and 23.9%, respectively. Stage III/IV tumors showed high *Fn* surface area expression (66.7%). *Fn* intratumoral heterogeneity (34.8%) was higher than that of KRAS (4.3%; $p < 0.001$) and BRAF (2.2%; $p < 0.001$). The Ki-67 index in *Fn*-positive cases was higher than that in negative cases (93.9% vs. 89.0%; $p = 0.01$).

Conclusions

Fn was strongly present in CRC superficial areas at stage III/IV. The presence of Fn in the deep areas of adjacent normal mucosa also increased. The intratumoral heterogeneity of *Fn* is important in the use of *Fn* as a biomarker, as *Fn* is associated with CRC proliferative capacity.

Keywords: *Fusobacterium nucleatum*; Colorectal cancer; Intratumoral heterogeneity

Introduction

Colorectal cancer (CRC) is the third most common cancer and the fourth most common cause of cancer death worldwide. Advances in genomic and molecular biology have elucidated some of the genetic mechanisms leading to colorectal carcinogenesis [1, 2], while treatment strategies considering the molecular background, such as KRAS/BRAF mutations, have improved patient survival [3, 4]. However, further elucidation of the mechanism of colorectal carcinogenesis is essential. A close relationship between CRC and *Fusobacterium nucleatum* (*Fn*) has been the focus of research [5]. *Fn*, a resident gram-negative aerobic bacterium, lives in the oral cavity, has been associated with periodontal disease, respiratory infections, cardiovascular disease, Alzheimer' s disease, inflammatory bowel disease, and several cancers [6]. In CRC, the same *Fusobacterium* species have been detected in primary CRC and liver metastasis tissues [7], and *Fn* has been significantly associated with chemoresistance and poor survival [8-10]. Therefore, *Fn* is expected to be used as a biomarker or treatment target for CRC [7, 11, 12].

Although whether *Fn* plays a causative role in CRC or is an outcome has not been confirmed, a role in the progression of CRC has been demonstrated [13]. The mechanism of *Fn* adhesion to CRC through the FadA-E-cadherin and Fap2-GalGalNAc pathways has been indicated [14, 15]. Given that the amount of *Fn* in stool increases continuously according to the cancer stage [16], it is reasonable to think that *Fn* derived from the stool affects CRC; however, the possibility of *Fn* derived from blood has also been considered [15]. To clarify these questions and elucidate *Fn* ecology, we analyzed the distribution of *Fn* in tissues, not stool, and analyzed tumor status, including histological and molecular factors in several stages of colorectal neoplasms, which included early stages of tumorigenesis, such as adenoma and early stage CRC resected by endoscopic mucosal resection (EMR) and endoscopic submucosal dissection (ESD), with matched adjacent normal mucosas. In addition, we compared *Fn* status of the "surface" and "deep" areas of advanced CRC and adjacent normal mucosa using surgically resected

cases. To confirm *Fn*'s use as a biomarker, we analyzed the heterogeneity of *Fn* presence in cancer tissue compared to KRAS/BRAF status, which is considered a universally prognostic biomarker in CRC. Moreover, we evaluated the Ki-67 index in these cancer tissues to confirm the proliferative role of *Fn* in CRC.

Methods

Materials

This study included 200 colorectal adenomas and cancers that were diagnosed and resected at Okayama University Hospital between January 2017 and December 2018. There were 95 cases of EMR, 52 cases of ESD, and 53 cases of surgical resection, respectively. In addition, 45, 49, and 51 matched normal-appearing adjacent mucosal tissues were also collected from each patient. In this study, tumor histology was classified according to the Vienna classification, and we regarded subgroup 4.2 "non-invasive carcinoma" as the cancer group (pathological Stage 0). Tumor staging was performed according to the Union for International Cancer Control (UICC). Patients with serrated lesions (hyperplastic polyps, sessile serrated lesions, and traditional sessile adenomas) have been excluded [17]. The clinicopathological features of this study are summarized in Table 1. A total of 118 cases were adenomas, while 82 cases were cancers. In the cancer cases, 23, 20, 17, 17, and 5 cases were diagnosed with stage 0, stage I, stage II, stage III, and stage IV disease, respectively. This study was approved by the Research Ethics Committee of Okayama University Hospital. Written informed consent was obtained from each patient prior to their inclusion in the study.

DNA extraction

Formalin-fixed paraffin-embedded (FFPE) CRC tissues, adenomas, and normal mucosa were used to extract genomic DNA using the QIAamp DNA FFPE Kit (Qiagen, Valencia, USA). In

46 out of 53 surgical cases, DNA was separately harvested from the "surface" and "deep" areas of both cancer tissue and matched adjacent normal mucosa to evaluate the molecular status and *Fn* presence (Supplemental Fig. 1). We defined the"deep area" as the lower half of the submucosa. DNA concentration was evaluated using a NanoDrop 2000 (Thermo Fisher Scientific, Waltham, USA).

Quantitative real-time polymerase chain reaction (qPCR) of *Fn*

We performed qPCR to measure the amount of *Fn* DNA in tissues. Custom-made primer/probe sets were used to amplify *Fn* and the reference human gene solute carrier organic anion transporter family number 2A1 (SLCO2A1). The primer and probe sequences were shown in Supplemental table 1. The PCR was performed in 20 μL reactions containing 30 ng of genomic DNA (2 μL), 1× final concentration Prime time gene expression Master Mix 2.0 (IDT, Coralville, USA) (10 μL), each Prime qPCR Assay (FAM/HEX) (1 μL), and deionized distilled water (6 μL). The DNA was amplified and detected with a Roche LightCycler 96® system (Roche, Basel, Switzerland) under the following conditions: 10 min at 95 °C and 45 cycles of 15 s at 95 °C and 1 min at 60 °C.

All specimens were analyzed in duplicate, and we regarded a specimen as "*Fn* positive" when both results were positive to exclude nonspecific PCR amplification. For the analysis of surgical tissues, if either the surface area or deep area of tissue was *Fn*-positive, we regarded the case as an *Fn*-positive case.

The amount of *Fn* DNA in each tissue was calculated by $2^{-\triangle Ct}$, where $\triangle Ct$ was the difference in the Ct value of *Fn* and SLCO2A1. The mean of the two Ct values for each reaction was used for analysis.

Digital PCR for KRAS/BRAF

KRAS and BRAF mutations were analyzed by droplet digital PCR (ddPCR) (QX200; Bio-

Rad, Hercules, USA) as described previously[18, 19]. The KRAS Screening Multiplex Kit (Bio-Rad, Hercules, USA) was used to detect KRAS mutations (G12A/C/D/R/S/V and G13D). The PrimePCR™ ddPCR Mutation Assay Kit BRAF V600E (Bio-Rad, Hercules, USA) was used to analyze BRAF mutations. Setting cutoff values in this study were 6000 on the x-axis (KRAS mutation) and 4000 on the y-axis (wild-type KRAS), and 2500 on the x-axis (BRAF mutation) and 2200 on the y-axis (wild-type BRAF). In addition to these cutoff values, we defined a KRAS mutation and a BRAF mutation if the fractional abundance of mutated alleles was > 1%.

Similar to *Fn*-positive cases, we defined a KRAS/BRAF mutation positive in surgical tissues, whose DNA was separately harvested from the surface and deep areas.

Assessment of the Ki-67 index

From FFPE blocks, 4 μm thick sections were cut. After standard deparaffinization, antigen retrieval was performed with Tris/ethylenediaminetetraacetic acid buffer (pH 9). Endogenous peroxidase was blocked with peroxidase-blocking solution (S2023; DAKO, Glostrup, Denmark) and the slides were incubated with a 1:60 dilution Ki-67 antibody (M7240; DAKO, Glostrup, Denmark). Secondary antibody incubation and signal development were performed in diaminobenzidine solution, according to the manufacturer's instructions (DAKO, Glostrup, Denmark).

The Ki-67 index was determined by calculating the percentage of tumor cells with positive staining among total number of at least 1500 tumor cells, by automated digital image analysis using Ventana Virtuoso image management software (Ventana, Tucson, USA), according to a previous report [20]. The three densest spots in each surface and deep area of 46 surgical cancer tissues were selected and analyzed by a researcher who was blind to the clinical and molecular information. The average value of the three indexes in each area was used for analysis.

Statistical analysis

The JMP version 14.0 software package (SAS Institute, Cary, NC, USA) was used for all statistical analyses. Continuous variables were expressed as the median and range, and assessed by the Student's *t*-test or nonparametric tests. The Pearson chi-squared test or Fisher's exact test was performed to compare categorical variables. We used the Wilcoxon rank sum test to compare relative abundances of *Fn* DNA and the Ki-67 index in each tissue. Differences were considered significant at a *p*-value of less than 0.05.

Results

Detection of *Fn* in CRC and adenoma

Fn in tissue from FFPE was detected in 44 (22%) cases from 200 CRCs and adenomas, and the presence was significantly higher in cancer (45.1%; 37/82) than in adenoma (5.9%; 7/118) ($p < 0.001$). The detection rate was correlated with pathological stage (pStage); 5.9% (7/118) in adenoma, 26.1% (6/23) in Stage 0, 35.1% (13/37) in stage I/II, and 81.8% (8/22) in stage III/IV, respectively (Fig. 1). Consistent with pStage, pathological T stage, N stage, and M stage were also associated with the presence of *Fn* (Table 1). The tumor size was significantly larger in the *Fn* positive group (median 30 mm; range 4-100 mm) than that in the negative group (median 8 mm; range 2-82 mm) ($p < 0.001$). Age, sex, and tumor location were not associated with the presence of *Fn*. The amount of tissue *Fn* DNA was also correlated with pStage (0/adenoma vs Ⅰ/Ⅱ, $p < 0.001$; 0/adenoma vs. III/IV, $p < 0.001$; Ⅰ/Ⅱ vs Ⅲ/Ⅳ, $p = 0.03$) (Supplemental Fig. 2).

Detection of *Fn* in matched adjacent normal mucosa of cancer and adenoma tissues

The detection rate of *Fn* in matched adjacent normal mucosa in cancer cases (26.6%; 21/79) was significantly higher than that in matched adjacent normal mucosa in adenoma cases (7.6%; 5/66)

(p = 0.003). In cancer cases, tumor tissue showed a higher presence of *Fn* compared to matched adjacent normal mucosa (p = 0.01), but not in adenoma cases. Additionally, the presence of *Fn* of normal mucosa in cancer cases was significantly higher than that of tumor tissue in adenoma cases (p < 0.001). **Fig. 1** demonstrates that the *Fn* detection rate in normal mucosa increased significantly only after reaching stage I/II, while there was no difference between stage I/II and III/IV cancer (27.8% vs. 40.9%, p = 0.3).

The amount of *Fn* in normal mucosa of cancer was significantly higher than that in adenoma (p < 0.001) (Supplemental Fig. 3), while the amount of *Fn* was significantly lower than that in cancer tissue of stage III/IV (p < 0.0001), with no difference in cancer tissue of stage I/II (p = 0.2) (Supplemental Fig. 4).

KRAS/BRAF mutations in CRC and adenoma

Of the 200 CRCs and adenomas, KRAS and BRAF mutations were detected in 49 (24.5%) and 10 cases (5%), respectively (Table 1). KRAS mutations were higher in the advanced stage (0/adenoma, 19.5%; Ⅰ/Ⅱ, 35.1%; III/IV, 40.9%; p = 0.02). Conversely, BRAF mutation was not correlated with pathological stage (0/adenoma: 5.0%, Ⅰ/Ⅱ: 2.7%, Ⅲ/Ⅳ: 9.1%; p = 0.6). In cancer cases, the location was associated with BRAF mutations (Right 12.8% vs. Left 0%; p = 0.02), but not with KRAS mutations (Right 41% vs. Left 32.6%; p = 0.42). There was no significant association between KRAS and BRAF mutations and the presence of *Fn*.

Detection of *Fn* on the surface and in deep areas of cancer/normal mucosa

In 46 out of 53 surgical cases, the *Fn* detection rate was 45.7% (21/46) on the surface of the tumor, 32.6% (15/46) in the deep area of the tumor, 26.1% (12/46) on the surface of adjacent matched normal mucosa, and 23.9% (11/46) in the deep area of adjacent matched normal mucosa. The cancer

surface area showed a high *Fn* presence compared to the surface and deep areas of normal mucosa ($p = 0.05$; $p = 0.03$, respectively), but the deep area of cancer did not show any difference from others (vs. surface area of cancer, $p = 0.20$; vs. surface area of normal mucosa, $p = 0.29$; and vs. deep area of normal mucosa, $p = 0.09$). Interestingly, these four groups did not show any difference in stage I/II, while the surface area of cancer in stage III/IV (66.7%) was significantly higher than that in the normal mucosa (23.8%, $p = 0.01$) and in the deep area of normal mucosa (28.6%, $p = 0.03$)(Fig. 2). The *Fn* detection rate in the deep area of cancer in stage III/IV (42.9%) was higher than that on the surface and in the deep area of normal mucosa; however, the difference was not statistically significant. **Fig. 3** shows the distribution of *Fn* in colorectal tissue. *Fn* grew markedly on the surface of stage III/IV tumors, and invaded the deep areas both in cancer tissue and adjacent normal mucosa.

Fn presence and KRAS/BRAF status between the surface and deep areas of surgical tissue

Table 2 shows *Fn* presence and the KRAS/BRAF status between the surface and deep areas of 46 surgical cases. The heterogeneity of *Fn* (34.8%, 16/46) was significantly higher than that of KRAS (4.3%, 2/46; $p = 0.0004$) and BRAF (2.2%, 1/46; $p < 0.0001$).

Ki-67 index and *Fn* status in surgical cancer tissues

The Ki-67 index was significantly higher on the surface of 46 surgical cancer tissues (93.5%) than in the deep area (89.2%) ($p = 0.02$). Among a total of 92 cancer areas, including the surface and deep areas of 46 surgical cancer tissues, the presence of *Fn* in tissues was significantly associated with a high Ki-67 index compared to the absence of *Fn* (93.9% vs. 89.0%; $p = 0.01$) (Fig. 4a). The presence of *Fn* was correlated with the Ki-67 index in the deep area of cancers (presence: 93.4% vs. absence: 85.4%; $p = 0.01$), but not for the surface area (presence: 94.5% vs. absence: 92.7%; $p = 0.28$) (Fig. 4b).

Discussion

In this study, we examined the presence of *Fn* in colorectal adenomas, cancers, and matched adjacent normal mucosa, and first analyzed the differentiation of the presence of *Fn* between the "surface" and "deep" areas of cancers and normal mucosa. This result helps to understand the ecology of *Fn* in colon tissues. The presence of *Fn* in tumor tissue increased significantly at the stage of noninvasive cancer, and also increased continuously according to the pathological stage. The presence of *Fn* in adjacent normal mucosa was low at the noninvasive cancer stage and increased to an extent in invasive cancer. Additionally, we revealed that *Fn* grew markedly on the surface area of stage III/IV tumors, and invaded the deep area both in cancer tissue and adjacent normal mucosa (Fig. 3). Moreover, our analysis revealed the heterogeneity of *Fn* in tumor tissue compared with the KRAS/BRAF status. This result indicated that we need to pay attention to how we evaluate *Fn* status, especially if *Fn* becomes a prognostic or refractory marker for chemotherapy in various cancers in the future. Analysis of the Ki-67 index in surgical tissues also validated the role of *Fn* in CRC proliferation.

Recent studies have shown a close relationship between *Fn* and CRC. The relative abundance of *Fn* in stool is significantly elevated from noninvasive cancer to more advanced stages by metagenomic and metabolomic analyses [16]; this result is remarkably similar to our analysis of tumor tissues. These results imply that *Fn* in the stool directly influences CRC. It is not yet clear whether *Fn* is a cause or consequence of CRC [21]; however, reasonable mechanisms of *Fn* affects CRC are indicated. Abed et al. identified that *Fn* Fusobacterial lectin (Fap2) protein plays an important role in CRC adherence by binding to Gal-GalNAc [15]. Gal-GalNAc is highly overexpressed in CRC compared to adenoma and normal tissues. Rubenstein et al. indicated that *Fn* adheres to CRC by binding E-cadherin with FadA, an adhesin molecule expressed on the surface of *Fn*; the binding results in the activation of the β-catenin signaling pathway promoting CRC proliferation [14]. In their subsequent research, a

positive feedback loop between FadA and the Wnt/β-catenin signaling pathway has been identified in cancerous cells, and absent in non-cancerous cells [13]. Kostic et al. indicated Fn generated a proinflammatory tumor-promoting microenvironment that was conductive for CRC progression [22]. From these reports and our study, we hypothesized that once premalignant adenoma develops into cancer caused by somatic mutations, *Fn* in the stool increases due to the influence of the tumor microenvironment, and adheres to and invades colorectal tissues, including normal mucosa, through Gal-GalNAc adhesion, particularly on the surface of cancer tissues[15]. In addition, increasing the binding between proliferating FadA and E-cadherin causes tumor progression in cancers, but not in adenomas [13].

Fn is expected to be a useful biomarker for patient prognosis and management of CRC. Several studies have shown that *Fn* is associated with recurrence, chemoresistance and shorter survival in CRC [8-10, 23]. Anti-*Fn* therapy is also expected [7, 24]. In our analysis, we revealed the heterogeneity of *Fn* in cancer tissues compared to KRAS/BRAF mutations. Interestingly, five cases showed an absence of *Fn* on the surface of cancer, while a presence of Fn in the deep areas. Intratumoral heterogeneity of biomarkers in several cancers has been shown to contribute to treatment failure and drug resistance [25, 26]. In CRC, some reports indicate the heterogeneity of KRAS mutations [27, 28]. However, the high homogeneity of the KRAS status analyzed by digital PCR in our study, which provides high sensitivity compared to previous studies, was considered a reliable result. To establish *Fn* as a predictive biomarker in the future, we need to recognize *Fn*'s intratumoral heterogeneity. This results in this study imply the inefficiency of biopsies from the surface area of CRC. The heterogeneity of *Fn* in CRC, such as the presence of Fn in the deep area of CRC, also may be associated with the resistance against chemotherapy. In addition, heterogeneity of *Fn*, contrary to the homogeneity of KRAS/BRAF status, may also show that *Fn* plays a role in exacerbating cancer progression after malignant transformation by somatic mutation.

We analyzed the Ki-67 index in 46 surgical cancer tissues to confirm the role of *Fn* in CRC progression. Ki-67 is a cell proliferation-associated nuclear marker, and several studies have shown that high Ki-67 expression is associated with poor overall survival in CRC [29]. *Fn*-positive cancer tissues showed a high Ki-67 index compared to *Fn*-negative tissues, demonstrating that *Fn* was closely correlated with cancer cell proliferation; this relationship may lead to poor prognosis in *Fn*-positive CRC. The relationship of *Fn* and CRC proliferation capacity had been discussed and proved with *in vivo* and *in vitro* experiments[13, 14, 22, 30]. Yang et al. found infection of CRC cells with *Fn* to increase their proliferation, invasive activity, and ability to form xenograft tumors in mice[30]. They revealed TLR4/ MYD88/ NFκB leading by *Fn* infection stimulated the overexpression of oncogenic miR21 in CRC. Although the mechanism of *Fn* and CRC proliferation is complex and still undetermined, activation of Wnt/β-catenin signaling, tumor-promoting microenvironment and TLR-4/NFκB were proved as one of its proliferating mechanism[13, 14, 22, 30]. Our study also support the relationship of *Fn* and CRC proliferation capacity.

Regarding the origin of *Fn* in colorectal tissues, similar to previous studies, we postulate that *Fn* in the stool affects CRC [16, 22, 31]. The identical strain of *Fn* were detected in colorectal cancer and saliva also supports this estimation[32]. However, it has also been discussed that blood-borne *Fn* is localized in CRC [15]. Thus, we performed a small pilot experiment using blood just before ESD obtained from 10 patients who were *Fn*-positive. qPCR using genomic DNA extracted from these blood samples did not show the presence of *Fn* in all cases. Although further larger studies using advanced cancer cases are required, our results, including this pilot experiment, may help to discern the origin of *Fn* in CRC.

The limitations of this study need to be mentioned. First, we used relatively recent FFPE tissues to maintain the accuracy of this experiment. Therefore, we could not verify *Fn* status as a

prognostic biomarker because of the short observation period. Second, our study focused on conventional adenomas that contribute to the main pathway of CRC carcinogenesis, and did not include serrated lesions, which indicate that the serrated pathway contributes to the development of 10% to 30% of all CRCs. Third, we could not collect the normal colorectal mucosa of healthy controls because of ethical issues, and the deep area of adjacent normal mucosa of adenoma/ stage 0 cancer was also unavailable because resected specimens did not include enough submucosa. However, based on a previous study [33], and the current study, we speculate that the presence of *Fn* in these tissues is quite low. Fourth, we could not prove the existence of Fn in CRC and normal mucosa pathologically. To ensure our findings, we need to further validation experiments.

In conclusion, we demonstrated a favorable relationship between *Fn* and CRC. Our detailed examination of how *Fn* exists in CRC and adjacent normal mucosa may support the theory that *Fn* in the stool plays a proliferating role in CRC. The heterogeneity of *Fn* in cancer tissue is important in the use of *Fn* status as a biomarker for cancer in the future; however, further data is needed.

Reference

1 Markowitz SD, Bertagnolli MM. Molecular origins of cancer: Molecular basis of colorectal cancer. *N Engl J Med* 2009; **361**: 2449-60.

2 Guinney J, Dienstmann R, Wang X *et al.* The consensus molecular subtypes of colorectal cancer. *Nat Med* 2015; **21**: 1350-6.

3 Dahabreh IJ, Terasawa T, Castaldi PJ, Trikalinos TA. Systematic review: Anti-epidermal growth factor receptor treatment effect modification by KRAS mutations in advanced colorectal cancer. *Ann Intern Med* 2011; **154**: 37-49.

4 Souglakos J, Philips J, Wang R *et al.* Prognostic and predictive value of common mutations for treatment response and survival in patients with metastatic colorectal cancer. *Br J Cancer* 2009; **101**: 465-72.

5 Lee SA, Liu F, Riordan SM, Lee CS, Zhang L. Global investigations of fusobacterium nucleatum in human colorectal cancer. *Front Oncol* 2019; **9**: 566.

6 Han YW. Fusobacterium nucleatum: a commensal-turned pathogen. *Curr Opin Microbiol* 2015; **23**: 141-7.

7 Bullman S, Pedamallu CS, Sicinska E *et al.* Analysis of Fusobacterium persistence and antibiotic response in colorectal cancer. *Science* 2017; **358**: 1443-8.

8 Yu T, Guo F, Yu Y *et al.* Fusobacterium nucleatum Promotes Chemoresistance to

Colorectal Cancer by Modulating Autophagy. *Cell* 2017; **170**: 548-63 e16.

9 Yamaoka Y, Suehiro Y, Hashimoto S *et al.* Fusobacterium nucleatum as a prognostic marker of colorectal cancer in a Japanese population. *J Gastroenterol* 2018; **53**: 517-24.

10 Mima K, Nishihara R, Qian ZR *et al.* Fusobacterium nucleatum in colorectal carcinoma tissue and patient prognosis. *Gut* 2016; **65**: 1973-80.

11 Ganesan K, Guo S, Fayyaz S, Zhang G, Xu B. Targeting Programmed Fusobacterium nucleatum Fap2 for Colorectal Cancer Therapy. *Cancers (Basel)* 2019; **11**.

12 Zhang X, Zhu X, Cao Y, Fang JY, Hong J, Chen H. Fecal Fusobacterium nucleatum for the diagnosis of colorectal tumor: A systematic review and meta-analysis. *Cancer Med* 2019; **8**: 480-91.

13 Rubinstein MR, Baik JE, Lagana SM *et al.* Fusobacterium nucleatum promotes colorectal cancer by inducing Wnt/beta-catenin modulator Annexin A1. *EMBO Rep* 2019; **20**.

14 Rubinstein MR, Wang X, Liu W, Hao Y, Cai G, Han YW. Fusobacterium nucleatum promotes colorectal carcinogenesis by modulating E-cadherin/beta-catenin signaling via its FadA adhesin. *Cell Host Microbe* 2013; **14**: 195-206.

15 Abed J, Emgard JE, Zamir G *et al.* Fap2 Mediates Fusobacterium nucleatum Colorectal Adenocarcinoma Enrichment by Binding to Tumor-Expressed Gal-GalNAc. *Cell Host Microbe* 2016; **20**: 215-25.

16 Yachida S, Mizutani S, Shiroma H *et al.* Metagenomic and metabolomic analyses reveal distinct stage-specific phenotypes of the gut microbiota in colorectal cancer. *Nat Med* 2019; **25**: 968-76.

17 Crockett SD, Nagtegaal ID. Terminology, Molecular Features, Epidemiology, and Management of Serrated Colorectal Neoplasia. *Gastroenterology* 2019; **157**: 949-66 e4.

18 Kinugasa H, Nouso K, Miyahara K *et al.* Detection of K-ras gene mutation by liquid biopsy in patients with pancreatic cancer. *Cancer* 2015; **121**: 2271-80.

19 Matsumoto K, Kato H, Nouso K *et al.* Evaluation of Local Recurrence of Pancreatic Cancer by KRAS Mutation Analysis Using Washes from Endoscopic Ultrasound-Guided Fine-Needle Aspiration. *Dig Dis Sci* 2020; doi: 10.1007/s10620-019-06006-6.

20 Kwon AY, Park HY, Hyeon J *et al.* Practical approaches to automated digital image analysis of Ki-67 labeling index in 997 breast carcinomas and causes of discordance with visual assessment. *PLoS One* 2019; **14**: e0212309.

21 Amitay EL, Werner S, Vital M *et al.* Fusobacterium and colorectal cancer: causal factor or passenger? Results from a large colorectal cancer screening study. *Carcinogenesis* 2017; **38**: 781-8.

22 Kostic AD, Chun E, Robertson L *et al.* Fusobacterium nucleatum potentiates intestinal tumorigenesis and modulates the tumor-immune microenvironment. *Cell Host Microbe* 2013; **14**: 207-15.

23 Ogino S, Nosho K, Irahara N *et al.* Lymphocytic reaction to colorectal cancer is associated with longer survival, independent of lymph node count, microsatellite instability, and CpG island methylator phenotype. *Clin Cancer Res* 2009; **15**: 6412-20.

24 Abed J, Maalouf N, Parhi L, Chaushu S, Mandelboim O, Bachrach G. Tumor Targeting by Fusobacterium nucleatum: A Pilot Study and Future Perspectives. *Front Cell Infect Microbiol* 2017; **7**: 295.

25 Gerlinger M, Swanton C. How Darwinian models inform therapeutic failure initiated by clonal heterogeneity in cancer medicine. *Br J Cancer* 2010; **103**: 1139-43.

26 Gerlinger M, Rowan AJ, Horswell S *et al.* Intratumor heterogeneity and branched evolution revealed by multiregion sequencing. *N Engl J Med* 2012; **366**: 883-92.

27 Richman SD, Chambers P, Seymour MT *et al.* Intra-tumoral heterogeneity of KRAS and BRAF mutation status in patients with advanced colorectal cancer (aCRC) and cost-effectiveness of multiple sample testing. *Anal Cell Pathol (Amst)* 2011; **34**: 61-6.

28 Jo P, Konig A, Schirmer M *et al.* Heterogeneity of KRAS Mutation Status in Rectal Cancer. *PLoS One* 2016; **11**: e0153278.

29 Luo ZW, Zhu MG, Zhang ZQ, Ye FJ, Huang WH, Luo XZ. Increased expression of Ki-67 is a poor prognostic marker for colorectal cancer patients: a meta analysis. *BMC Cancer* 2019; **19**: 123.

30 Yang Y, Weng W, Peng J *et al.* Fusobacterium nucleatum Increases Proliferation of Colorectal Cancer Cells and Tumor Development in Mice by Activating Toll-Like Receptor 4 Signaling to Nuclear Factor-kappaB, and Up-regulating Expression of MicroRNA-21. *Gastroenterology* 2017; **152**: 851-66 e24.

31 Suehiro Y, Sakai K, Nishioka M *et al.* Highly sensitive stool DNA testing of Fusobacterium nucleatum as a marker for detection of colorectal tumours in a Japanese population. *Ann Clin Biochem* 2017; **54**: 86-91.

32 Komiya Y, Shimomura Y, Higurashi T *et al.* Patients with colorectal cancer have identical strains of Fusobacterium nucleatum in their colorectal cancer and oral

cavity. *Gut* 2019; **68**: 1335-+.

33 McCoy AN, Araujo-Perez F, Azcarate-Peril A, Yeh JJ, Sandler RS, Keku TO. Fusobacterium is associated with colorectal adenomas. *PLoS One* 2013; **8**: e53653.

Table 1 Clinicopathological and molecular features with *Fn* status

	All patients N=200	*Fn* negative N=156 (78%)	*Fn* positive N=44 (22%)	P- value
Age (mean, range)	69 (39-91)	69 (40-90)	68 (39-91)	0.80
Sex: male	125 (62.5%)	103 (66.0%)	22 (50%)	0.07
Tumor location				0.86
Right	105 (52.5%)	81 (51.9%)	24 (54.5%)	
Left	95 (47.5%)	75 (48.1%)	20 (45.5%)	
Size (mean, range)	13(2-100)	8 (2-82)	30 (4-100)	<0.0001
pT stage				<0.0001
Adenoma	118 (59.0%)	111 (71.2%)	7 (15.9%)	
Tis	23 (11.5%)	17 (10.9%)	6 (13.6%)	
T1	17 (8.5%)	12 (7.7%)	5 (11.4%)	
T2	9 (4.5%)	4 (2.6%)	5 (11.4%)	
T3	31 (15.5%)	11 (7.1%)	20 (45.5%)	
T4	2 (1%)	1 (0.6%)	1 (2.3%)	
pN stage				<0.0001
0	180 (90%)	152 (97.4%)	28 (63.6%)	
1/2	20 (10%)	4 (2.6%)	16 (36.4%)	
pM stage				0.032
0	195 (97.5%)	155 (99.3%)	40 (90.9%)	
1	5 (2.5%)	1 (0.6%)	4 (9.1%)	
pStage				<0.0001
Adenoma	118 (59.0%)	111 (71.2%)	7 (15.9%)	
0	23 (11.5%)	17 (10.9%)	6 (13.6%)	
Ⅰ	20 (10%)	14 (9.0%)	6 (13.6%)	
Ⅱ	17 (8.5%)	10 (6.4%)	7 (15.9%)	
Ⅲ	17 (8.5%)	3 (1.9%)	14 (31.8%)	
Ⅳ	5 (2.5%)	1 (0.6%)	4 (9.1%)	
KRAS mutation	49 (24.5%)	35 (22.4%)	14 (31.8%)	0.20
BRAF mutation	10 (5%)	6 (3.8%)	4 (9.1%)	0.23
Treatment				<0.0001
EMR/ESD/OPE	95/52/53	92/40/24	3/12/29	

Fn, Fusobacterium.nucleatum; EMR, endoscopic mucosal resection; ESD, endoscopic submucosal dissection; OPE, operation

Table 2

Fn/KRAS/BRAF status between surface and deep area of surgical tissue

N=46	*Fn*				KRAS				BRAF			
	Homogeneity		Heterogeneity		Homogeneity		Heterogeneity		Homogeneity		Heterogeneity	
Surface	+	-	+	-	Mut	Wild	Mut	Wild	Mut	Wild	Mut	Wild
Deep	+	-	-	+	Mut	Wild	Wild	Mut	Mut	Wild	Wild	Mut
	10	20	11	5	15	29	2	0	1	44	1	0

Fn, Fusobacterium.nucleatum; Surface, Surface area of surgical tissue; Deep, Deep area of surgical tissue; +, positive; -, negative; Mut, mutation

Figure Legend

Fig. 1 Detection rate of *Fn* in tumor tissues and adjacent normal mucosa in colorectal adenoma and CRC according to each tumor stage. (*$p < 0.05$, **$p < 0.001$) *Fn*, *Fusobacterium nucleatum*; CRC, colorectal cancer Statistical analyses were performed using the Pearson chi-squared test or Fisher's exact test

Fig. 2 Detection rate of *Fn* on the surface and in the deep areas of cancer tissue and adjacent normal mucosa in 46 surgical cases according to each tumor stage. (*$p < 0.05$, **$p < 0.001$) *Fn*, *Fusobacterium nucleatum* Statistical analyses were performed using the Pearson chi-squared test or Fisher's exact test

Fig. 3 Graphical representation of the presence of *Fn* in tumor tissue and adjacent normal mucosa during multistep CRC progression. *Fn*, *Fusobacterium nucleatum*; CRC, colorectal cancer

Fig. 4 (a) Ki-67 index with the presence or absence of *Fn* in the 92 areas overall from 46 surgical cancer tissues, including the surface and deep areas of each tissue. (b) Ki-67 index with the presence or absence of *Fn* according to the surface and deep areas in 46 surgical cancer tissues. *Fn*, *Fusobacterium nucleatum* (*$p < 0.05$) Statistical analyses were performed using the Wilcoxon rank sum test

Supplemental Fig. 1 Surface and deep area of CRC tissues and matched adjacent normal mucosa. CRC, colorectal cancer

Supplemental Fig. 2 The amount of Fn DNA in tumor tissue according to each tumor stage. (*$p <$

0.05, **p < 0.001) *Fn*, *Fusobacterium nucleatum* Statistical analyses were performed using the Wilcoxon rank sum test

Supplemental Fig. 3 The amount of Fn DNA in adjacent normal mucosa of adenoma and cancer (*p < 0.05, **p < 0.001) *Fn*, *Fusobacterium nucleatum* Statistical analyses were performed using the Wilcoxon rank sum test

Supplemental Fig. 4 The amount of *Fn* DNA in adjacent normal mucosa of cancer and cancer tissue according to each stage. (**p < 0.001) *Fn*, *Fusobacterium nucleatum* Statistical analyses were performed using the Wilcoxon rank sum test

Supplemental Table.1 Primer and probe sequence.

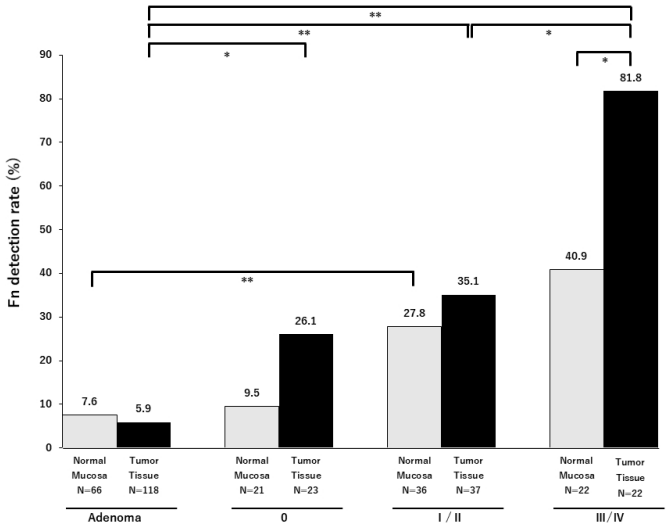

Fig. 1 Detection rate of Fn in tumor tissues and adjacent normal mucosa in colorectal adenoma and CRC according to each tumor stage.

54x30mm (600 x 600 DPI)

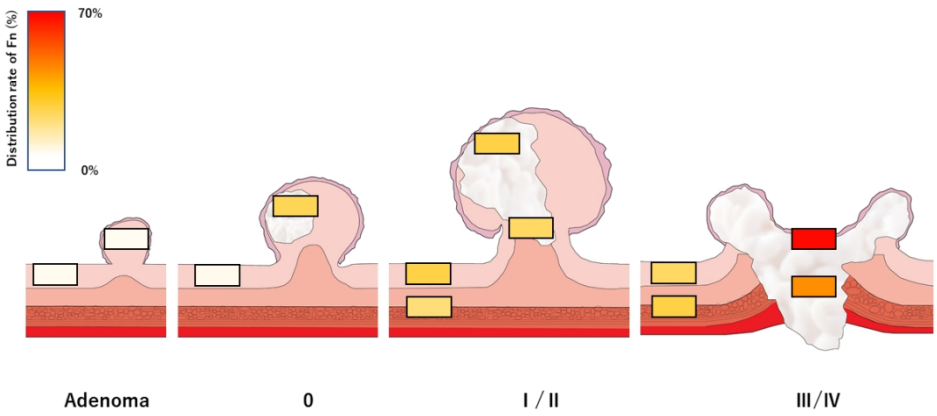

Fig. 3 Graphical representation of the presence of Fn in tumor tissue and adjacent normal mucosa during multistep CRC progression.

108x60mm (300 x 300 DPI)

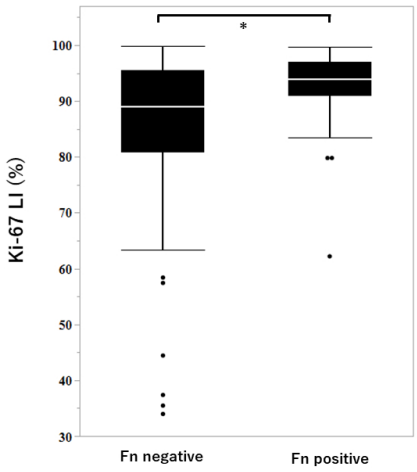

Fig. 4 (a) Ki-67 index with the presence or absence of Fn in the 92 areas overall from 46 surgical cancer tissues, including the surface and deep areas of each tissue.

54x30mm (600 x 600 DPI)

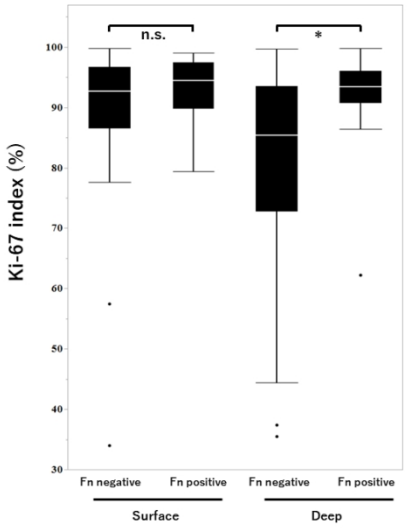

Fig. 4 (b) Ki-67 index with the presence or absence of Fn according to the surface and deep areas in 46 surgical cancer tissues.

54x30mm (600 x 600 DPI)

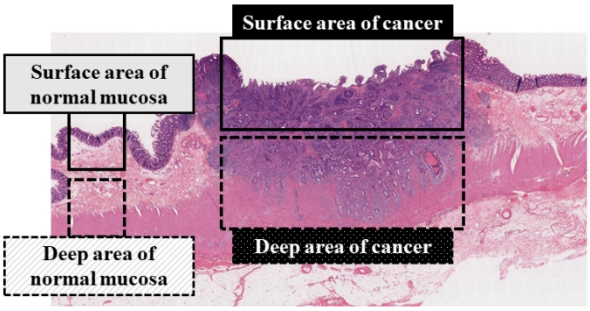

Supplemental Fig. 1 Surface and deep area of CRC tissues and matched adjacent normal mucosa.

108x60mm (300 x 300 DPI)

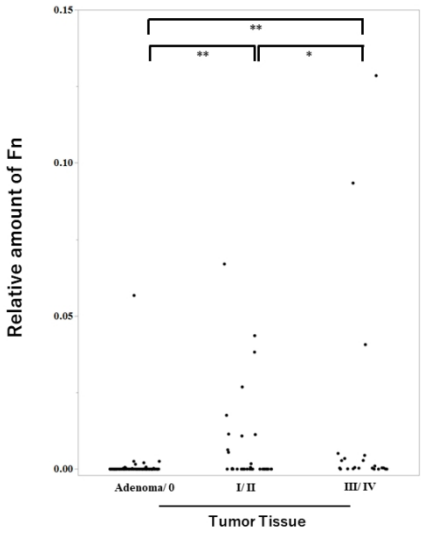

Supplemental Fig. 2 The amount of Fn DNA in tumor tissue according to each tumor stage.

108x60mm (300 x 300 DPI)

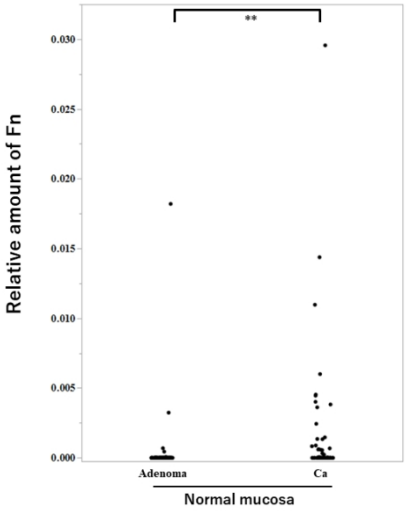

Supplemental Fig. 3 The amount of Fn DNA in adjacent normal mucosa of adenoma and cancer.

54x30mm (600 x 600 DPI)

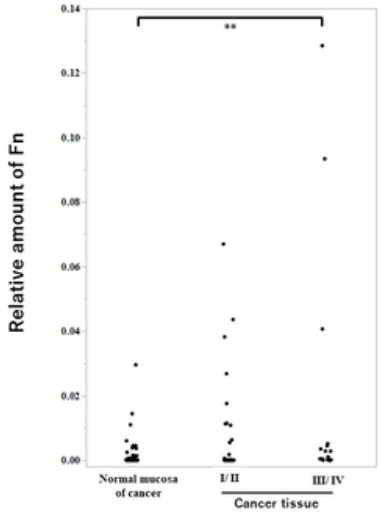

The amount of Fn DNA in adjacent normal mucosa of cancer and cancer tissue according to each stage.

54x30mm (300 x 300 DPI)

Supplemental Table 1　Pirmer and probe sequence

Gene: Primer/ Probe	Sequence (5′-3′)
Fusobacterium nucleatum Forward primer	5′- CAACCATTACTTTAACTCTACCATGTTCA-3′
Fusobacterium nucleatum Reverse primer	5′-GTTGACTTTACAGAAGGAGATTATGTAAAAATC-3′
Fusobacterium nucleatum Probe	5′-GTTGACTTTACAGAAGGAGATTA-3′
SLCO2A1 Forward primer	5′-ATCCCCAAAGCACCTGGTTT-3′
SLCO2A1 Reverse primer	5′-AGAGGCCAAGATAGTCCTGGTAA-3′
SLCO2A1 Probe	5′-CCATCCATGTCCTCATCT-3′